Communications to the Editor

Conducting Polymer-Based Electrodeless Deposition of Pt Nanoparticles and Its Catalytic Properties for Regioselective Hydrosilylation Reactions

Hung-Hsin Shih,[†] Darrick Williams,[§] Nathan H. Mack,[‡] and Hsing-Lin Wang*[,†]

Physical Chemistry and Spectroscopy Group, Chemical Diagnostics and Engineering Group, and Center for Integrated Nanotechnologies, Los Alamos National Laboratory, Los Alamos, New Mexico 87544

Received October 2, 2008
Revised Manuscript Received November 25, 2008

There has been increasing interests in fabricating metal nanoparticle (MNP) conducting polymer composites due to their potential applications toward biosensors,[1,2] catalysts,[3] and electrocatalysts.[4] Polyaniline (PANI) is a commonly used conducting polymer known for its low cost, facile synthesis, and environmental stability. PANI exhibits unique redox potentials with three distinct redox states that can be easily controlled via electrochemical and chemical methods. These properties suggest PANI as an ideal substrate for the synthesis of MNP/PANI composites via electrodeless deposition techniques. Current work in this area has been limited in their study of the catalytic properties of the resulting MNP/PANI composites prepared through either electrochemical synthesis[5] or blending the nanoparticles with conducting polymers.[6,7] One promising method for making a Pt nanoparticle/PANI composite is through the sequential electrochemical deposition of a PANI film followed by reduction of Pt salt, resulting in a thick composite with high Pt nanoparticles loading. O'Mullane et al. demonstrated a two-step chemical method by mixing a PANI solution with a Pt salt in a cosolvent (formic acid) to form a Pt/PANI nanoparticle composite with Pt ranging in size from 30 to 90 nm. Subsequent immersion of this composite film in a K_2PtCl_4 solution leads to formation of homogeneously dispersed Pt nanoparticles with sizes ranging from 1 to 2 nm.[8] The greatly enhanced Pt surface area of this smaller size distribution gives rise to superior electrocatalytic characteristics. Understanding the integral nature of the role the PANI substrate has in the formation of Pt particles is important with respect to controlling and potentially improving the catalytic performance of the polymer nanocomposites.

This work aims at demonstrating the controlled fabrication of Pt nanoparticles with different surface coverages and growth patterns on a PANI membrane that is comprised of a dense top polymer layer and a porous substructure.[9] We observe significant differences in the morphology of the deposited Pt particles, depending on the nature (doped/undoped) of the PANI surface (see Scheme 1).

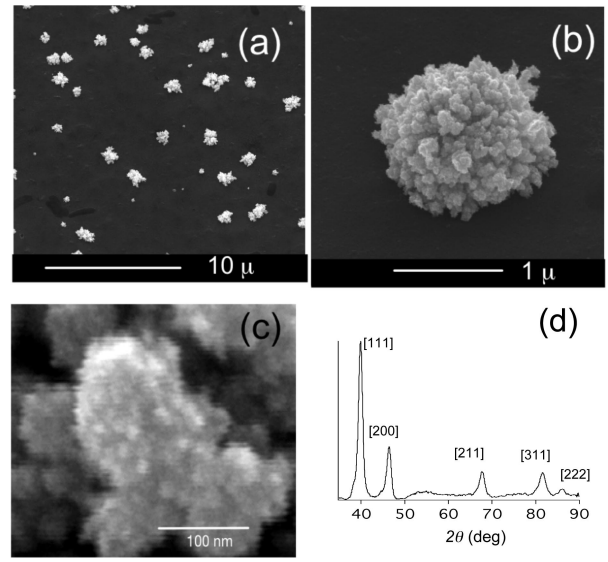

Figure 1. SEM micrograph of dispersed Pt particles on a doped PANI membrane surface (a). Magnified image of a Pt particle exhibiting a fractal growth pattern (b). High-resolution SEM image of a Pt particle aggregate (c). XRD pattern of the Pt particles (d).

Scheme 1. Molecular Structure of Doped and Undoped PANI

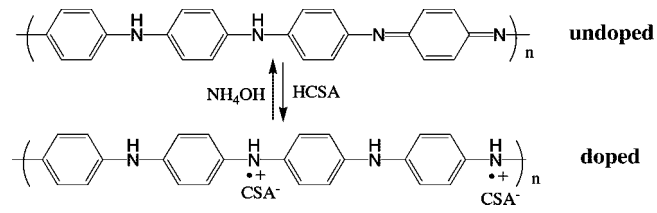

Figure 1 shows the growth of Pt particles on the surface of camphorsulfonic acid-doped PANI. These particles are highly dispersed on the PANI surface with very limited surface coverage. XRD (Rigaku Ultima III) of these Pt particles shows the diffraction pattern of Pt metal. Using the full width at half-maximum (fwhm) of the XRD peak, we can estimate the particle size to be ∼7.4 nm. This result is consistent with the fact that, upon close examination of the large particles with high-resolution SEM, we find that they are conglomerates of many small (<10 nm) nanoparticles (Figure 1c). These aggregates have a fractal-like pattern that is similar to that of fractal structures derived from simulation studies based on the diffusion-limited aggregation (DLA) model.[10,11] The DLA model predicts a hit-and-stick mechanism in which random movement of Pt molecules toward nucleation sites on the PANI surface results in fractal growth patterns. The agreement of these structures with simulations suggests a growth mechanism wherein $PtCl_4^{2-}$ ions approach the PANI surface, bind to a suitable reduction site where the Cl^- ions dissociate and the Pt^{2+} ion is subsequently reduced to Pt metal without significant diffusive effects. These Pt nanoparticles serve as nucleation sites for subsequent

* To whom correspondence should be addressed.
[†] Physical Chemistry and Spectroscopy Group.
[‡] Chemical Diagnostics and Engineering Group.
[§] Center for Integrated Nanotechnologies.

10.1021/ma802219z CCC: $40.75
Published on Web 12/15/2008

Scheme 2. Hydrosilyation Reactions of Internal Para- and Ortho-Substituted Aryl Alkynes

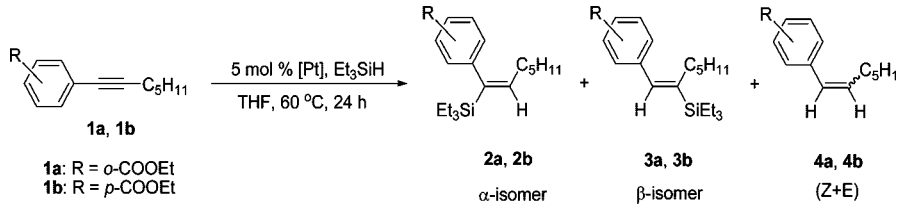

reduction of $PtCl_4^{2-}$ ions, resulting in the final fractal-like structure. In contrast to these fractal-like Pt particles, when on an undoped PANI surface, the resulting Pt nanoparticles grown have a significantly altered morphology (Figure 2). The $PtCl_4^{2-}$ ions reduced by the undoped PANI result in a much higher coverage of Pt particles on the PANI surface, with an increasing thickness of the Pt nanoparticle layer with increasing time. The SEM image reveals the Pt layer to be composed of smaller densely packed particles with a sheetlike morphology. The fwhm of the XRD peaks suggests a particle size of ~9.7 nm, consistent with the thickness of the nanosheets revealed by the high-resolution SEM (inset of Figure 2a).

The drastic difference in surface coverage and structure between the Pt particles on doped and undoped PANI surfaces is attributed to changes in surface chemistry and structure homogeneity of the polymer that result from doping PANI with a protonic acid.[12] The doped PANI results in highly aggregated Pt particles that are scarcely populated on the PANI membrane surface, while the undoped PANI membrane is fully covered with sheetlike Pt particles. This suggests two very different growth mechanisms are present, which are sensitive to the surface chemistry of PANI membrane. In the initial stages of particle formation, the $PtCl_4^{2-}$ ions readily form a complex with secondary amines and tertiary imines on the PANI backbone (see Scheme 1). Here the dissociated Cl^- ions are assumed to act as spectrator ions and not significantly affect Pt^{2+} ion reduction. In the case of the doped PANI, the majority of the secondary amines and tertiary imines are occupied (protonated) by the dopants and therefore have a limited ability to bind Pt cations at the PANI surface. The few amines that are available as nucleation sites for particle growth are presumably dispersed over the polymer surface and directly correlate with the low surface coverage of the aggregate particles. These data suggest that Pt nanoparticle growth can be intrinsically modified to select for differences in surface coverage, particle size, and morphology simply based on the doping level of PANI substrate.

Electronic spectra of the PANI substrate are indicative of the oxidation state of the polymer and can be used to follow the reduction of Pt ions. The UV−vis spectrum of a 0.1 μm PANI thin film that was spin-cast on a glass substrate show significant spectral shifts after immersion in a 100 mM aqueous $PtCl_4^{2-}$ solution for 2 h (see Supporting Information). The two absorption peaks at 630 and 330 nm in the pristine PANI film are consistent with the emeraldine base form of the polymer, while the blue-shifted peaks at 570 and 320 nm after exposure to Pt ions are consistent with the formation of the pernigraniline base, the fully oxidized form of polyaniline.[13,14] This result clearly shows that PANI acts as the reductant responsible for converting Pt^{2+} into zerovalent Pt metal and supports the observation that the surface chemistry of the PANI directly influences the structure and morphology of the resulting metal particles.

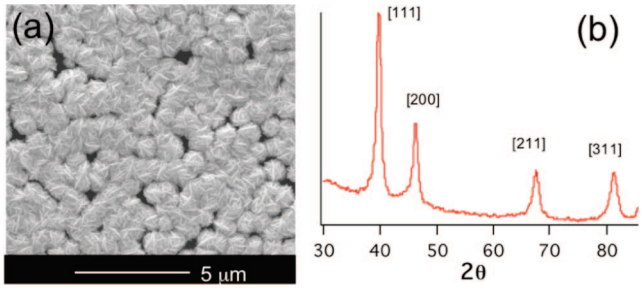

Figure 2. SEM micrograph of Pt particles on an undoped PANI surface (a). Inset is a high-resolution image of (a) illustrating sheetlike morphology. XRD pattern of the Pt particles (b).

These large morphological differences in the observed Pt particles for these two preparations may have impacts on the catalytic performance of the MNP/PANI nanocomposites. To examine these effects, the regioselective hydrosilyation reactions of internal para- and ortho-substituted aryl alkynes (**1a**, **1b**) with Et_3SiH were selected as model catalytic reactions (Scheme 2). Analyses of these two reacted solutions are listed in Table 1 and show that both **1a** and **1b** were completely converted to greater than 83% enatiomeric excess of the α-isomer with a combined yield of greater than 95% (see Supporting Information). Similar yields were found using a commercially available Pt/C hydrosilylation catalyst; however, regioselectivity was severely reduced for **2b**. Although relatively slow compared to the commercially available Pt/C hydrosilyation catalyst, the Pt nanoparticle/PANI nanocomposites exhibit enhanced regioselectivity and excellent yields. The relative catalytic efficiency of Pt particles on doped vs undoped PANI is essentially identical, presumably because the nanoparticle size and the surface morphologies are comparable in relation to the size of the catalytically active sites on the Pt metal surface.

In summary, we have demonstrated a facile synthesis of Pt nanoparticles on PANI surfaces with control over the metal morphology and surface coverage by varying the polymer's surface chemistry. A DLA-based growth mechanism for these particles leads to drastic morphological differences depending upon the PANI doping level. The Pt nanoparticle decorated PANI exhibits excellent catalytic properties toward hydrosilylation of substituted aryl alkynes, suggesting their use in novel catalytic membrane reactor designs.

Acknowledgment. The authors thank the financial support from Laboratory Directed Research and Development (LDRD) fund under the auspices of DOE, BES Office of Science, the National Nanotechnology Enterprise Development Center (NNEDC), and the LANL Agnew Postdoctoral Fellowship. This work was performed in part at the U.S. Department of Energy, Center for Integrated Nanotechnologies, at Los Alamos National Laboratory (Contract DE-AC52-06NA25396) and Sandia National Laboratories (Contract DE-AC04-94AL85000).

Supporting Information Available: Detailed procedures for preparing polyaniline membranes via a phase inversion process; ^{1}H NMR spectra of compounds **1a**, **1b**, **2a**, and **2b**; UV/vis absorption spectra of polyaniline thin films before and after chemical deposition of Pt nanoparticles. This material is available free of charge via the Internet at http://pubs.acs.org.

References and Notes

(1) Kim, J. H.; Cho, J. H.; Cha, G. S.; Lee, C. W.; Kim, H. B.; Paek, S. H. *Biosens. Bioelectron.* **2000**, *14* (12), 907–915.
(2) Adhikari, B.; Majumdar, S. *Prog. Polym. Sci.* **2004**, *29* (7), 699–766.
(3) Gao, Y.; Chen, C.-A.; Gau, H.-M.; Bailey, J. A.; Akhadov, E.; Williams, D.; Wang, H.-L. *Chem. Mater.* **2008**, *20* (8), 2839–2844.
(4) Qi, Z. G.; Pickup, P. G. *Chem. Commun.* **1998**, (21), 2299–2300.
(5) Niu, L.; Li, Q. H.; Wei, F. H.; Chen, X.; Wang, H. *Synth. Met.* **2003**, *139* (2), 271–276.
(6) O'Mullane, A. P.; Dale, S. E.; Day, T. M.; Wilson, N. R.; Macpherson, J. V.; Unwin, P. R. *J. Solid State Electrochem.* **2006**, *10* (10), 792–807.
(7) Corbierre, M. K.; Cameron, N. S.; Sutton, M.; Mochrie, S. G. J.; Lurio, L. B.; Ruhm, A.; Lennox, R. B. *J. Am. Chem. Soc.* **2001**, *123* (42), 10411–10412.
(8) O'Mullane, A. P.; Dale, S. E.; Macpherson, J. V.; Unwin, P. R. *Chem. Commun.* **2004**, (14), 1606–1607.
(9) Wang, H. L.; Gao, J. B.; Sansinena, J. M.; McCarthy, P. *Chem. Mater.* **2002**, *14* (6), 2546–2552.
(10) Meakin, P. *Phys. Rev. Lett.* **1983**, *51* (13), 1119–22.
(11) Witten, T. A.; Meakin, P. *Phys. Rev. B: Condens. Matter* **1983**, *28* (10), 5632–42.
(12) Gao, J. B.; Sansinena, J. M.; Wang, H. L. *Chem. Mater.* **2003**, *15* (12), 2411–18.
(13) Cao, Y. *Synth. Met.* **1990**, *35* (3), 319–32.
(14) Huang, W. S.; Macdiarmid, A. G. *Polymer* **1993**, *34* (9), 1833–45.

MA802219Z